Earthquakes and Structures, *Vol. 15, No. 3 (2018) 319-334*
DOI: https://doi.org/10.12989/eas.2018.15.3.319

Effects of the isolation parameters on the seismic response of steel frames

Ahmet H. Deringöl*[1] and Huseyin Bilgin[2a]

[1]*Department of Civil Engineering, Gaziantep University, 27310, Gaziantep, Turkey*
[2]*Department of Civil Engineering, Epoka University, Tirana, Albania*

(Received June 21, 2017, Revised June 30, 2018, Accepted July 18, 2018)

Abstract. In this paper, an analytical study was carried out to propose an optimum base-isolated system for the design of steel structures equipped with lead rubber bearings (LRB). For this, 5 and 10-storey steel moment resisting frames (MRFs) were designed as Special Moment Frame (SMF). These two-dimensional and three-bay frames equipped with a set of isolation systems within a predefined range that minimizes the response of the base-isolated frames subjected to a series of earthquakes. In the design of LRB, two main parameters, namely, isolation period (T) and the ratio of strength to weight (Q/W) supported by isolators were considered as 2.25, 2.5, 2.75 and 3 s, 0.05, 0.10 and 0.15, respectively. The Force-deformation behavior of the isolators was modelled by the bi-linear behavior which could reflect the nonlinear characteristics of the lead-plug bearings. The base-isolated frames were modelled using a finite element program and those performances were evaluated in the light of the nonlinear time history analyses by six natural accelerograms compatible with seismic hazard levels of 2% probability of exceedance in 50 years. The performance of the isolated frames was assessed in terms of roof displacement, relative displacement, interstorey drift, absolute acceleration, base shear and hysteretic curve.

Keywords: base isolation; lead rubber bearing; moment resisting frame; non-linear analysis; structural response control

1. Introduction

Despite many of the advances in earthquake engineering, a large number of the current existing building stock in earthquake-prone countries were built using techniques and code provisions which are below the current standards (Bilgin 2013). Undoubtedly, most of these structures need to be rehabilitated if the catastrophic consequences to be avoided in future earthquakes. As the time and financial resources will be an obstacle to rehabilitate all these structures in a proper time interval, many of these facilities might be damaged in the event of a strong earthquake. Due to the growing awareness of vulnerable cities in parallel to the urbanization in earthquake-prone countries in different parts of the world and the consequent seismic risk, engineering community has shown significant progress in the development and application of innovative systems for seismic protection. One of the effective ways of reducing seismic demand on both structural and non-structural parts of the construction is based on the structural control through new base isolation technologies. The common feature of these recently proposed approaches is the adjustment of the dynamic interaction between the severe ground motion characteristics and the superstructure to minimize the vibrations and thereby, preserve the structure from severe damage. Structural response control can be achieved by either the modification of the inherent dynamic characteristics or the modification of the energy dissipation capacity of the structure. In the first approach, the period of the structure is shifted away from the main dominant period of the earthquake input leading to avoid from resonance phenomena. In the latter case, energy dissipation capacity of the structure is enlarged by introducing proper devices (Naeim and Kelly 1999). Due to the reduction of the input energy, an improved response with respect to the traditional ways of constructions is achieved during severe ground shakings, with substantial reduction of story accelerations, interstorey drifts and stresses on structural members. A variety of base isolation systems have been proposed to mitigate the devastating effects of the earthquakes on building structures over the past three decades. Those can be grouped into two parts; namely the sliding systems and elastomeric bearings. The sliding systems are proposed to minimize the seismic energy utilizing flexible interface material and restrain the transmission of the seismic force. The elastomeric bearing generally consists of three types; namely laminated rubber bearing, lead rubber bearing and high damping rubber bearing (Gur and Mishra 2013). Further, the lead rubber bearing consists of many rubber materials providing the flexibility while it has lead core for immense hysteretic dissipation and initial rigidity to sustain moderate seismic excitation such as wind and minor earthquakes (Jangid 2007).

The popularity of these systems for the base isolation of the structures has been increased particularly after Kobe earthquake (1995) (Fujita 1998). Many researchers have analytically and experimentally studied the response of the base isolation systems. For instance, Liang *et al*. (2002) also studied the wind-induced response of the base-isolated frames, especially for the tall buildings. The results showed

*Corresponding author, Ph.D. Student
E-mail: aderingol@gmail.com
[a]Associate Professor

http://www.techno-press.com/journals/eas&subpage=7
ISSN: 2092-7614 (Print), 2092-7622 (Online)

that the base-isolated tall buildings were very susceptible to wind storms. In the study of Kulkarni and Jangid (2003), the effects of the structure rigidity on the different base isolation systems such as elastomeric and sliding bearings were assessed by conducting rigid and flexible model. Moreover, Fragiacomo *et al*. (2003) proposed a simple design procedure that utilized the optimum design parameter of the isolation systems such as mass, strength, elastic and plastic stiffness. The linear analyses were performed under different ground motions and the analyses results showed that the maximum relative displacement and input energy dramatically reduced. Matsagar and Jangid (2004) also studied the seismic response of the multi-storey structure equipped with a different hysteretic model of the base isolation system. The effectiveness of the base-isolated structure was notably influenced by the variation of the system parameters such as isolator yield displacement, isolation time period and the number of storey. In the analytical study of the Jangid (2007), the seismic performance of the base-isolated structures (buildings and bridges) was assessed through time history analysis within six different near field records. The optimum yield strength of the isolator and period was preferred to reduce the roof storey absolute acceleration and isolator displacement at the same time. The minimum response of the acceleration and displacement was obtained when the ratio of the yield strength over the structure weight selected between 10%-15%. Providakis (2008) carried out pushover analysis on the seismic response of steel–concrete composite buildings isolated by LRB and evaluated the effect of the isolator height with setting three different cases for the composite buildings. Furthermore, the optimum design parameters of the isolator should be computed to surmount the acceleration and displacement response of the buildings. Alhan and Sürmeli (2011) investigated both linear and nonlinear base-isolated structures which were idealized for various isolation period and distributed the stiffness over the height of four different shear buildings and 3D representation. Those were subjected to five different real earthquake records. At the end of the analysis, a comprehensive discussion was presented whether the results of the shear building reliable or not with respect to the 3D model concerning the seismic performance criteria. Alhan and Şahin (2011) also examined the effect of structures flexibility, damping ratio and type of isolation models on the base isolation systems, hence three different storey level buildings were subjected to near-fault records of five different earthquakes. As expected, the flexible isolated structures caused greater storey acceleration than rigid isolated structures. Although the smaller yield strength brought about to drop on the storey acceleration, the variation of the isolation period had no consistent effect. Moreover, a numerical study was carried out to compare the response of two models considering three specified base isolation parameters (namely the normalized yield force, damping ratio, friction coefficient and isolation period) through non-stationary random earthquake motion. The acceleration response of the isolated structures escalated by increasing of the yield force and damping ratio while it did not vary with seismic frequency. In the study of Özdemir and Akyüz (2012), 7-storey reinforced concrete base-isolated buildings subjected to bi-directional excitations of the near-field ground motions were studied to show the variation of the floor accelerations in the base-isolated structures as a function of the design properties of the isolation system. Khoshnudian and Motamedi (2013) carried out time history analysis to emerge the effect of the strongest component of the selected excitations on the seismic behaviour of the asymmetric 4-storey base-isolated steel building. This building was supported with elastomeric bearing with various isolation periods, damping ratios and different level of eccentricities. The analysis results show that the effect of the isolation periods was greater than the damping ratio. Besides the isolators with higher period and lower damping ratio caused minimum energy dissipation. When the eccentricity was increased energy dissipation of the isolators were also reduced. Das and Mishra (2014) proposed an extensive study on the development of the lead rubber bearing by using an advanced material, remarkable hysteretic behavior and lesser yield displacement as the distinctive feature of the base isolation systems; thus Shape Memory Alloy Rubber Bearing (SMARB) was presented as the modified version of Lead Rubber Bearing. The supremacy of SMARB over the traditional LRB was performed by the nonlinear random ground motions. The results reported that the conventional LRB caused greater acceleration than SMARB. Furthermore, SMARB revealed more efficiency than LRB when the period of the isolator increased. Nigdeli *et al*. (2014) proposed an optimization method to equate the optimum seismic response. For this reason, some isolation system parameters such as displacement, damping ratio and period of the isolator determined as optimization restrictions and the 4-storey base-isolated frame were evaluated under near-fault and far fault earthquake records. The effectiveness of the optimized base isolation systems was checked by comparing with fixed-base structure considering the displacement and acceleration response. Liu *et al*. (2014) proposed a comprehensive study with regard to the three equivalent models assessed by time history analysis and the optimal damping ratio computed by a genetic algorithm. When considered the maximum displacement and the isolation period of other models, the proposed model achieved to acquire the presumed LRB displacement less than 5% error. Chun and Hur (2015) analytically and experimentally studied the effect of the variation of the isolation period and stiffness ratio for 15-storey base-isolated reinforced concrete frame. As an analytical model, the bilinear model was used to represent the actual characteristics of LRB, additionally the results of the analytical study were verified by setting up a shaking table test on the model scaled one-tenth. The results showed that the interstorey drift and roof storey acceleration responses were reduced by 33% and 65%, respectively with respect to the fixed base frame. In the study of Özdemir and Bayhan (2015), the 3-storey steel frame was equipped with three different LRB and then isolated steel frame was exposed to bi-directional near field records. A variety of nonlinear analysis was carried out to describe the deteriorating and non-deteriorating behavior of LRB. At the end of conducted bounding analysis, the

isolator displacement demand was obtained. The deteriorating and non-deteriorating hysteresis was compared with each other. Das *et al*. (2015) studied the effect of the normalized yield strength and period of the isolator on the response of 5-storey base-isolated shear building. The variation of the design parameters on the base-isolated structure through optimization process was further verified under sets of five real recorded earthquake ground motions. In the numerical study of Etedali and Sohrabi (2016), an extensive range of the isolator periods, eccentricity ratios, and the number of storey were presumed to assess the effect of the seismic behavior of the base-isolated structures with respect to the fixed base. The results affirmed that the base isolators remarkably reduce the torsional motion of storey especially in small eccentricities. Additionally, minimum of eccentricity (10%) caused the minimum displacement while the maximum of eccentricity (30%) caused maximum displacement. Alhan and Davas (2016) studied the seismic performance of structures supported with the base isolation systems of various characteristics under near-fault ground motions. The results showed that the optimum isolation parameters such as lower period with higher damping satisfied the reduction of the storey acceleration. Vasiliadis (2016) studied on 3-storey r.c. frames equipped with LRB and friction pendulum by three real seismic records. The efficiency of investigated isolation systems was tuned according to the ratio of the period of the isolated frames to fixed-base frames. The seismic performance of each isolated frames presented in terms of storey acceleration, drift and shear forces.

The main aims of the study are to (i) examine the seismic performance of the steel frames isolated by LRB, (ii) show the effectiveness of the base isolation systems against seismic excitation, (iii) study the variation of the isolation parameters of the LRB for 5 and 10-storey MRFs with different isolation systems, and (iv) emerge the optimum parameters of the LRB for minimum seismic response of the isolated system under earthquake records. In the light of the previous researchers, 5- and 10-storey steel MRFs designed as SMF and equipped with LRBs having different design properties such as isolation period, T, and characteristic strength to weight ratio, Q/W, in accordance with the code specification of ASCE (2005) and these isolated frames were analyzed using six natural accelerograms compatible with seismic hazard levels of 2% probability of exceedance in 50 years. The organization of the present study is as follows: the analytical modeling details of the frames including the original frames and base-isolated frames are given in Section 2. Additionally, the design parameters of the base isolation systems were given. The information on the earthquake records that are representatives of 2% probability of exceedance in 50 years was described. Then, the results of the nonlinear analysis were elaborately discussed in Section 3. Finally, the conclusions inferred from the analysis results are presented in a comparative manner in Section 4.

2. Analytical modeling of frames

MRFs are structural systems in which the resistance to

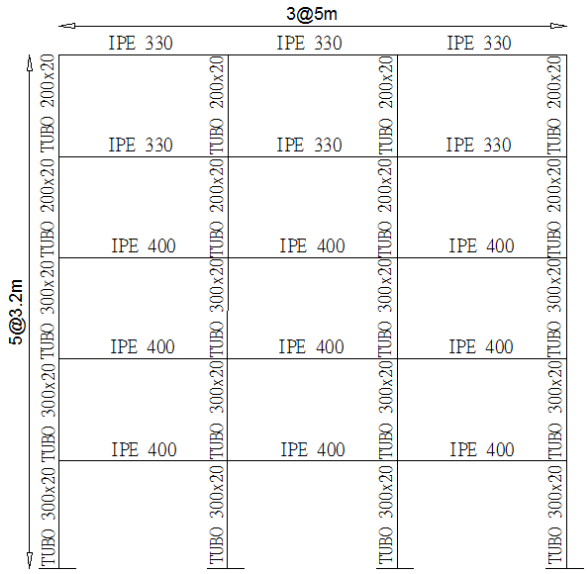

Fig. 1 Elevation views of 5-storey SMF (Asgarian *et al.* 2010)

lateral and gravity loadings are provided by the rigid frame action. The AISC (1997) and FEMA 350 (2000) seismic provisions defined three types of MRFs namely OMF, IMF and SMF. Asgarian *et al* (2010) designed 5 and 10-storey frame as a bare frame. However, in this study only SMF of 5 and 10-storey frames were selected and modified as base-isolated frames. The values of response modification factor (R) considered in the design of the SMF was 10 (Asgarian *et al*. 2010). Moreover, inelastic rotation capacity of SMF is specified 0.03. All of the bays have the same width of 5 m. Storey height is the same for all storey as 3.2 m. Elevation views of 5 and 10-storey frames were given in Figs. 1-2. The columns have all the same type, equal to square TUBE, altering their sections as shown in Figs. 1-2.

The fundamental periods of vibration of 5 and 10-storey SMF were obtained as 0.82 s and 1.55 s, respectively. Further details regarding the characteristics of the frames were elaborately explained by Asgarian *et al.* (2010). To represent the actual behavior of MRFs, rigid diaphragm and panel zones were assigned. For the nonlinear behavior of the frames, plastic hinges were determined and lumped plasticity approach was followed according to ASCE (2006) and FEMA 356 (2000). Analytical models of all frames were developed using nonlinear finite element program Sap2000 (CSI, 2011) which is capable of performing nonlinear static and dynamic analyses. In this study; the elastomeric Lead Rubber Bearings (LRB) are used in the base-isolated frames. LRB generally consists of many steel plates located at the top and bottom of the bearing, many alternating layers of elastomers and steel shims and in the middle lead core (Fig. 3) (Hameed *et al*. 2008).

The elastomeric material is designed for the lateral flexibility with the isolation component, the lead core utilizes the energy dissipation, while the inner steel shims carry the vertical load capacity of the bearing. The steel shims, together with the top and bottom steel fixing plates, also confines the central lead core. When the earthquake subjects to the structure, the lead core starts to yield and the

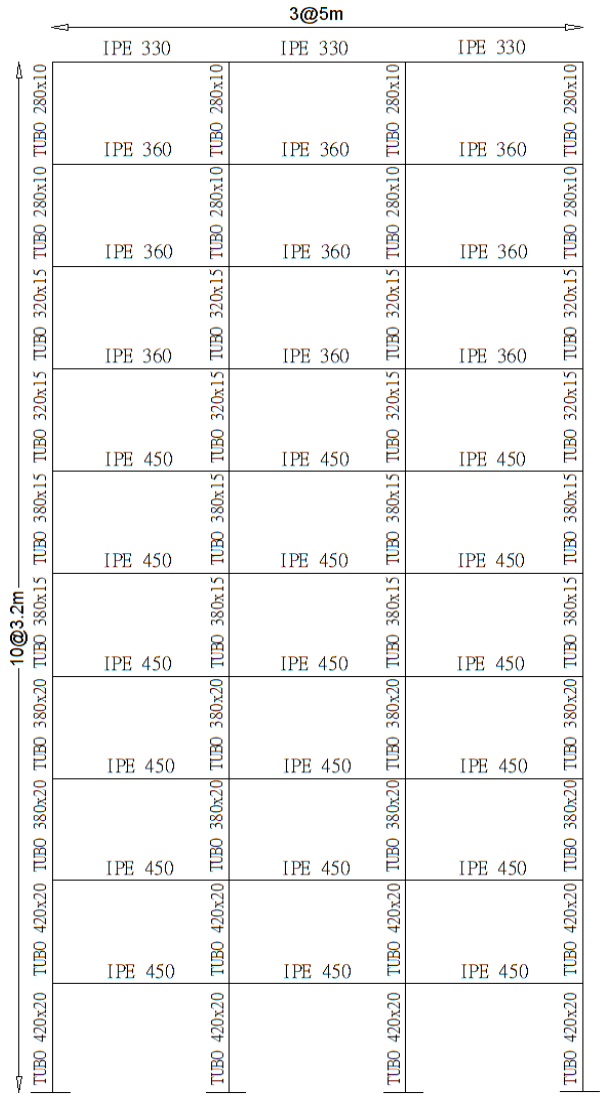

Fig. 2 Elevation views of 10-storey SMF (Asgarian *et al.* 2010)

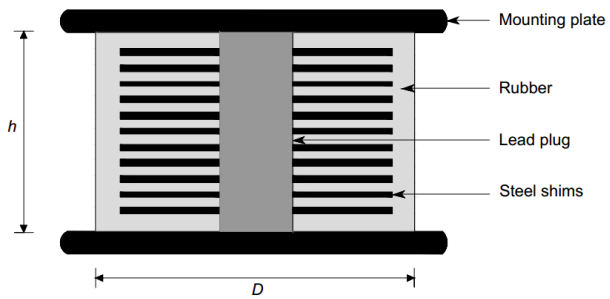

Fig. 3 Typical configuration of LRB (Hameed *et al.* 2008)

rubber layer also deforms laterally by shear deformation, both providing the movement of the structure horizontally and growing the energy dissipation (ASCE 1998).

It can be assumed that LRB consists of two models: (i) a linear viscoelastic element represented by the rubber, and (ii) a linear elastic-perfectly plastic element stimulated by the lead plug (Jerome, 2002). These models assume that the response relationship is bilinear, as indicated in Fig. 4 (Ozdemir and Constantinou 2010).

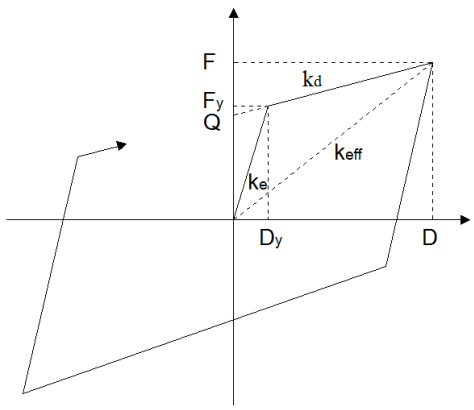

Fig. 4 The lead-plug bearing hysteresis of LRB (Ö zdemir and Constantinou 2010)

Design parameter of LRB was computed by an iterative solution following ASCE (2005). After assuming for the maximum isolator displacement, the iteration started and continued until the assumed and obtained values were almost the same. In the iterative procedure described in ASCE (2005), the following equations were used.

The assumed value of displacement D was then used to calculate the effective stiffness, k_{eff}

$$k_{eff} = k_d + \frac{Q}{D} \tag{1}$$

post-yield stiffness of the isolator, k_d

$$k_d = \frac{W.4\pi^2}{g.T^2} \tag{2}$$

effective damping, β_{eff}

$$\beta_{eff} = \frac{4Q.(D - D_y)}{2\pi.k_{eff}.D^2} \tag{3}$$

effective period, T_{eff}

$$T_{eff} = 2\pi\sqrt{\frac{W}{k_{eff}.g}} \tag{4}$$

displacement of isolation, D

$$D = \frac{g.S_a.T_{eff}^{\ 2}}{B.4\pi^2} \tag{5}$$

and yield strength, F_y

$$F_y = Q + k_d.D_y \tag{6}$$

where Q is the characteristic strength, T is target period assumed as 2.25, 2.5, 2.75 and 3 s (more than three times of fixed base), W is the total weight on the isolator, g is the gravitational force, B is damping reduction factor, D_y is yield displacement and S_a is spectral acceleration. Q/W defines three different characteristics force ratios (5%, 10%, and 15%). These ratios are essential to cover a wide range of isolation parameters with four different isolation periods. Although Naeim and Kelly (1999) proposed a constant value for the ratio of post-yield stiffness to initial stiffness (k_e), Ryan and Chopra (2004) recommend fixing the yield displacement instead of fixing k_e/k_d and their suggestion is

Table 1 The properties of LRB for outer and inner columns in 5-storey base-isolated frame systems

T (s)	Q/W	F_y (kN)	k_e (kN/m)	k_d (kN/m)	D (m)	k_{eff} (kN/m)	k_d/k_e	Q (kN)	β_{eff} (%)	Location
2.25	0.05	13.5	1355.8	185.8	0.389	215.9	0.14	11.7	8.6	Outer
	0.10	25.3	2525.8	185.8	0.179	316.6	0.07	23.4	24.8	
	0.15	36.9	3695.8	185.8	0.057	801.6	0.05	35.1	40.3	
	0.05	25.8	2578.4	353.4	0.389	410.6	0.14	22.3	8.6	Inner
	0.10	48.1	4803.4	353.4	0.179	601.9	0.07	44.5	25.0	
	0.15	70.3	7028.4	353.4	0.059	1480.9	0.05	66.8	42.0	
2.5	0.05	13.2	1320.5	150.5	0.480	174.9	0.11	11.7	8.7	Outer
	0.10	24.9	2490.5	150.5	0.221	255.9	0.06	23.4	25.6	
	0.15	36.6	3660.5	150.5	0.069	655.6	0.04	35.1	43.5	
	0.05	25.1	2511.2	286.2	0.479	332.7	0.11	22.3	8.7	Inner
	0.10	47.4	4736.2	286.2	0.220	488.1	0.06	44.5	25.8	
	0.15	69.6	6961.2	286.2	0.069	1241.2	0.04	66.8	44.6	
2.75	0.05	12.9	1294.4	124.4	0.580	144.6	0.10	11.7	8.6	Outer
	0.10	24.6	2464.4	124.4	0.262	213.7	0.05	23.4	24.8	
	0.15	36.3	3634.4	124.4	0.075	586.8	0.03	35.1	40.3	
	0.05	24.6	2461.6	236.5	0.580	274.9	0.10	22.3	8.7	Inner
	0.10	46.9	4686.6	236.5	0.262	406.4	0.05	44.5	25.1	
	0.15	69.2	6911.6	236.5	0.076	1109.2	0.03	66.8	41.9	
3.0	0.05	12.8	1274.6	104.5	0.689	121.5	0.08	11.7	8.7	Outer
	0.10	24.5	2444.6	104.5	0.310	180.1	0.04	23.4	25.6	
	0.15	36.2	3614.6	104.5	0.088	499.6	0.03	35.1	43.5	
	0.05	24.2	2423.8	198.8	0.688	231.1	0.08	22.3	8.7	Inner
	0.10	46.5	4648.8	198.8	0.312	341.4	0.04	44.5	25.7	
	0.15	68.8	6873.8	198.8	0.085	984.1	0.03	66.8	44.8	

Table 2 Properties of the ground motion records

Earthquake Record	Station	Year	Magnitude (M_w)	Mechanism	R_{jb} (km)	R_{rup} (km)	V_{s30} (m/s)	PGA(g)	PGV (cm/s)	PGD (cm)
Gazlı	Karakyr	1976	6.8	Unknown	3.9	5.5	659.6	0.59	64.94	24.18
Superstition Hills	Poe Road	1987	6.54	Strike-Slip	0.9	0.9	348.7	0.41	106.74	50.54
San Salvador	GeotechInvestig	1986	5.8	Strike-Slip	2.1	6.3	545.0	0.84	62.23	10.01
Cape Mendocino	Petrolia	1992	7.01	Reverse	0	8.2	712.8	0.61	81.87	25.48
Chi-Chi	TCU065	1999	7.62	Reverse-Oblique	0.6	0.6	305.9	0.82	127.80	93.22
Northridge	Sylmar-Olive	1994	6.69	Reverse	0	5.3	251.2	0.79	93.29	53.29

10 mm for LRBs. LRB was designed by a generic bi-linear hysteretic force-deformation relation as shown in Fig. 4 (Ö zdemir and Constantinou 2010). The isolation periods of 2.25, 2.5, 2.75 s and 3.0 s and the corresponding yield levels of Q/W are chosen, 5.0%, 10.0%, and 15.0% to cover a wide range of isolation system characteristics. Other properties of the isolation systems were calculated using Eqs. (1)-(6) and presented in Table 1 for 5-story frames, respectively. In this study, each isolation systems were labeled based on their isolation periods and yield levels (Q/W ratios) as to use in figures and throughout the rest of the text. For example, T3QW5 denotes an isolation system with T=3 s and Q/W=0.05. Typical isolation system parameters were presented in Table 1, where T ranges from 2.25 to 3 s and Q/W from 0.05 to 0.15. For the base-isolated models, two different bearings (inner and outer) were designed according to the vertical loads on the column. Designed LRBs were placed under each column of all examined models that include rubber isolator as a nonlinear link element employed by Park *et al.* (1986). Typical elevation view of 5-storey frames with LRB was represented in Fig. 5. Thus, twelve different isolation

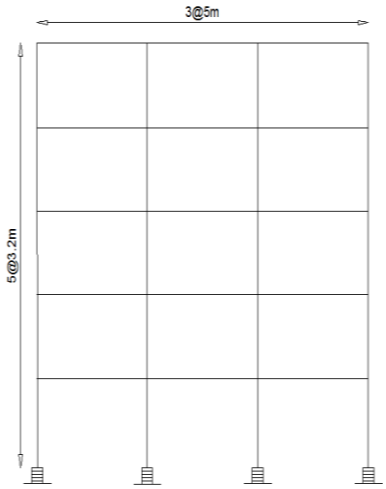

Fig. 5 The elevation view of 5-storey SMF with LRB

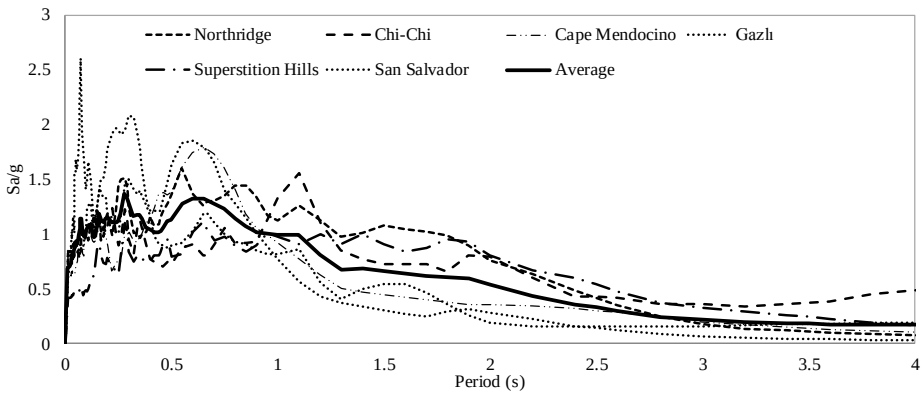

Fig. 6 5% Damped elastic acceleration response spectra of the ground motions

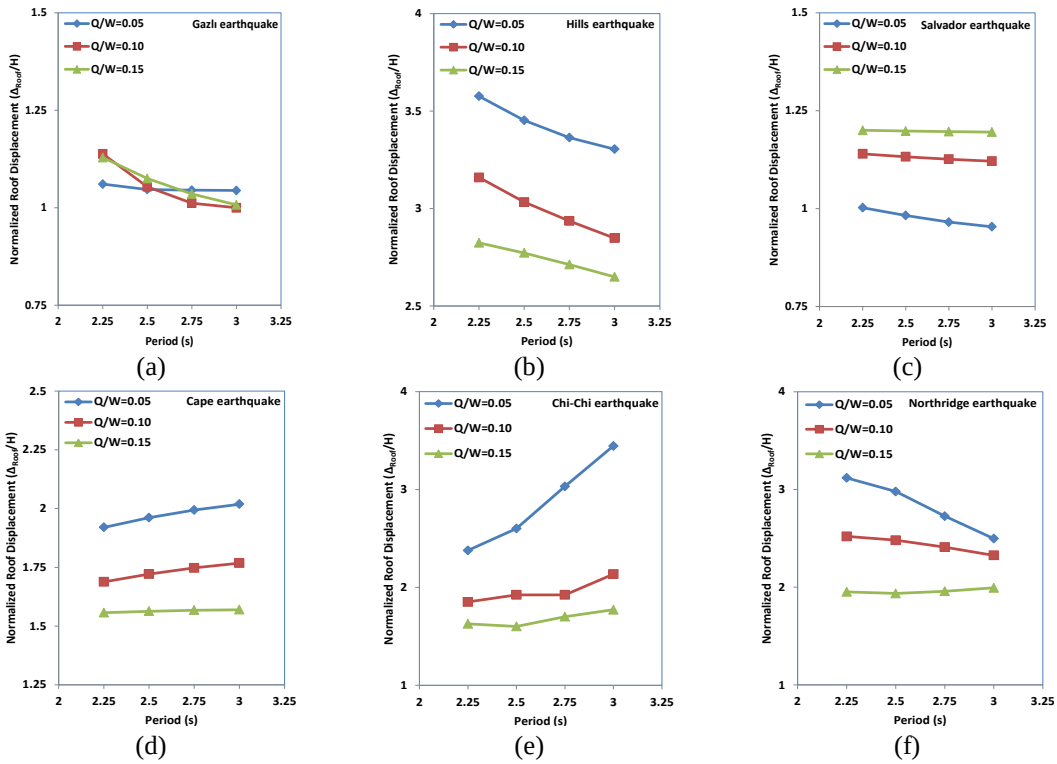

Fig. 7 Variation of normalized roof displacements with isolation period and damping of 5-storey SMF under earthquakes

systems with different characteristics were considered in this study. For 5 and 10-storey SMF as base isolation systems, lead rubber bearings were applied to each base support and denoted by LRB. The analytical models of the considered cases were developed and nonlinear time history analyses were conducted using the finite element program of Sap2000 (CSI 2011) non-linear version 14. In the nonlinear time history analysis inertial forces were determined from the ground motions and the response of the building either in deformations or forces calculated as a function of time including six natural accelerograms. It should be noted that in the scaling process the mean code spectra or a set of earthquakes should be as close as possible to the mean spectrum. The purpose of doing this is to have the accelerograms of the six earthquakes scaled to approximately the same intensity level such that the responses can be represented. For the time history analyses six natural accelerograms compatible with seismic hazard levels of 2% probability of exceedance in 50 years with details given in Table 2. The seismic ground motions used in the nonlinear analysis provided from the strong motion database of Pacific Earthquake Engineering Research Centre (PEERC 2011). Their 5% damped elastic acceleration response spectra are presented in Fig. 6.

3. Discussion of results

The present study assessed the dynamic characteristic and seismic response of 5 and 10-storey MRFs equipped with LRBs having different design properties such as isolation period, *T*, and characteristic strength to weight ratio, *Q/W*. The inelastic seismic response of the base-isolated frames has been examined in terms of roof displacement, roof absolute acceleration, relative displacement, interstorey drift ratio, base shear, hysteretic

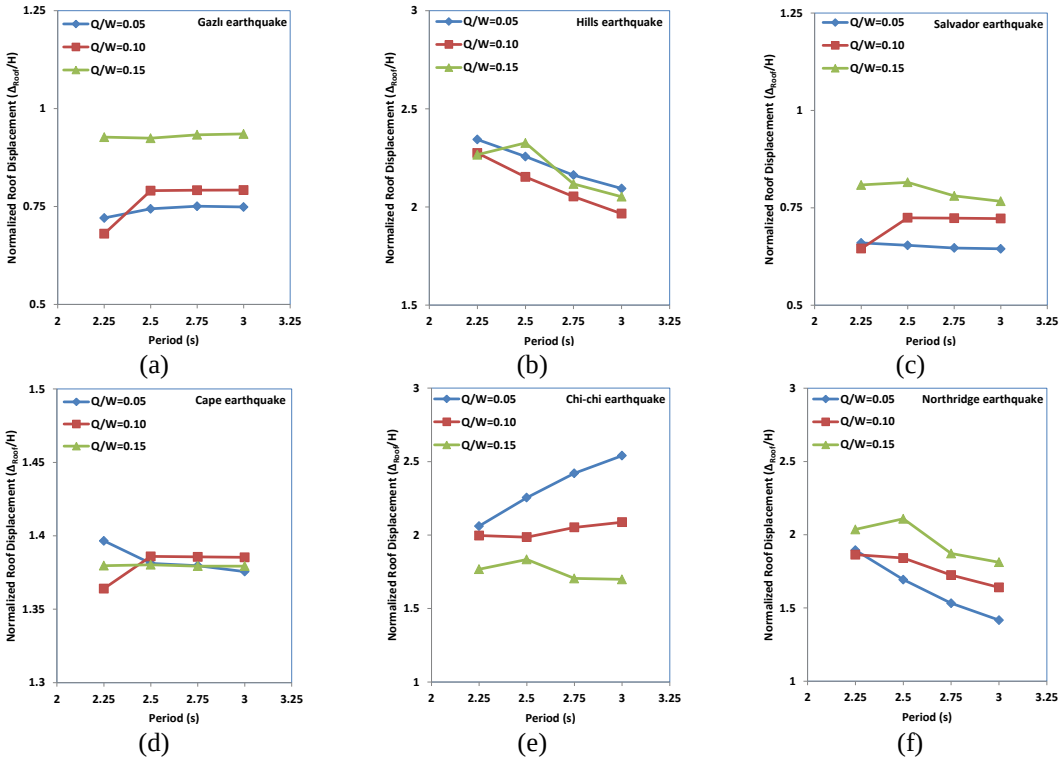

Fig. 8 Variation of normalized roof displacements with isolation period and damping of 10-storey SMF under earthquakes

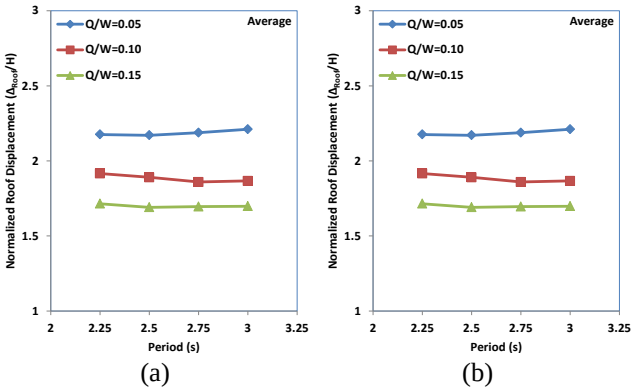

Fig. 9 Variation of average normalized roof displacements of 5-storey SMF (left) and 10-storey SMF (right)

curve and dissipated energy obtained through nonlinear analysis.

3.1 Roof displacement

The roof displacement demand of the 5 and 10-storey isolated frames with predefined isolation period and yield strength ratio under six ground motions were determined and normalized by the building height to remove the effect of the shape factor. The normalized roof displacement demand of the examined frames was given in Figs. 7-8. Furthermore, the variation of the average normalized roof displacement was plotted in Fig. 9. It can be clearly seen that the frames supported with the LRB having different isolation parameters had successfully reduced the roof displacement demand especially under Hills and Northridge earthquake as shown in Figs. 7(b) and 8(f), respectively. In addition to the yield strength ratio and isolation period, characteristic of the earthquakes and number of stories also had a notable effect on the variation of the roof displacement. For example, increasing the isolation period seemed to reduce the roof displacements, similarly increasing *Q/W* ratio also caused great reduction in the roof displacements with respect to the other isolation systems (see Fig. 7). Moreover, the various adverse trends were experienced in the normalized roof displacement when 5 and 10-storey base-isolated frames subjected to Chi-chi earthquake as shown in Figs. 7(e) and 8(e). For instance, the isolation system of T3QW5 led to 3.45 of normalized roof displacement while it was reduced up to 1.77 by T3QW15 for 5-storey base-isolated frame. It can also be verified that T3QW15 caused minimum average normalized roof displacement response for both frames as shown in Fig. 9. It was observed that when the yield strength ratio fixed and the isolation period was shifted from 2.25 s to 3 s (see Fig. 9) the average normalized roof displacement was generally decreased parallel to descending trend of the isolator stiffness as shown in Table 1. Similarly, it was generally reduced when the isolation period was constant, and the yield strength ratio was changed from 0.05 to 0.15. Simultaneously 10-storey SMF leads to lower values for the normalized roof displacement.

3.2 Roof absolute accelerations

The variation of average roof absolute accelerations versus storey height was plotted in Fig. 10, the average roof absolute accelerations neither monotonically enhance over the height of the frames nor remain constant. They initially reduce towards mid-height and then quickly escalate

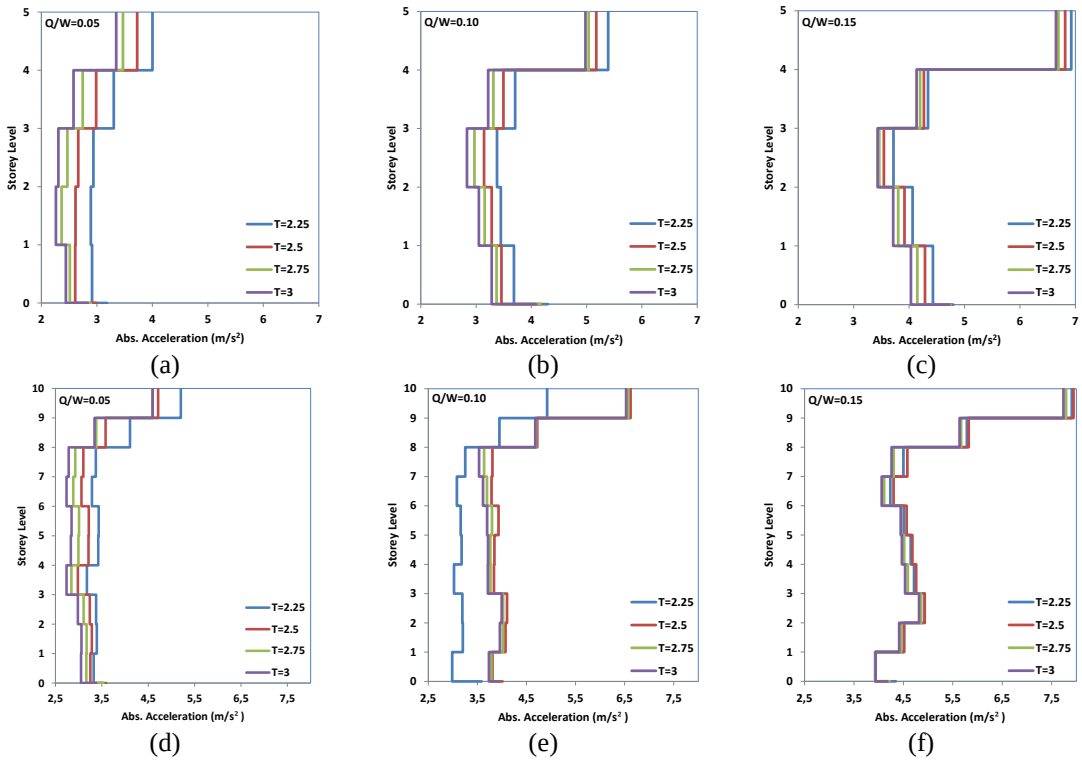

Fig. 10 Variation of average absolute acceleration against storey height of 5-storey SMF and 10-storey SMF

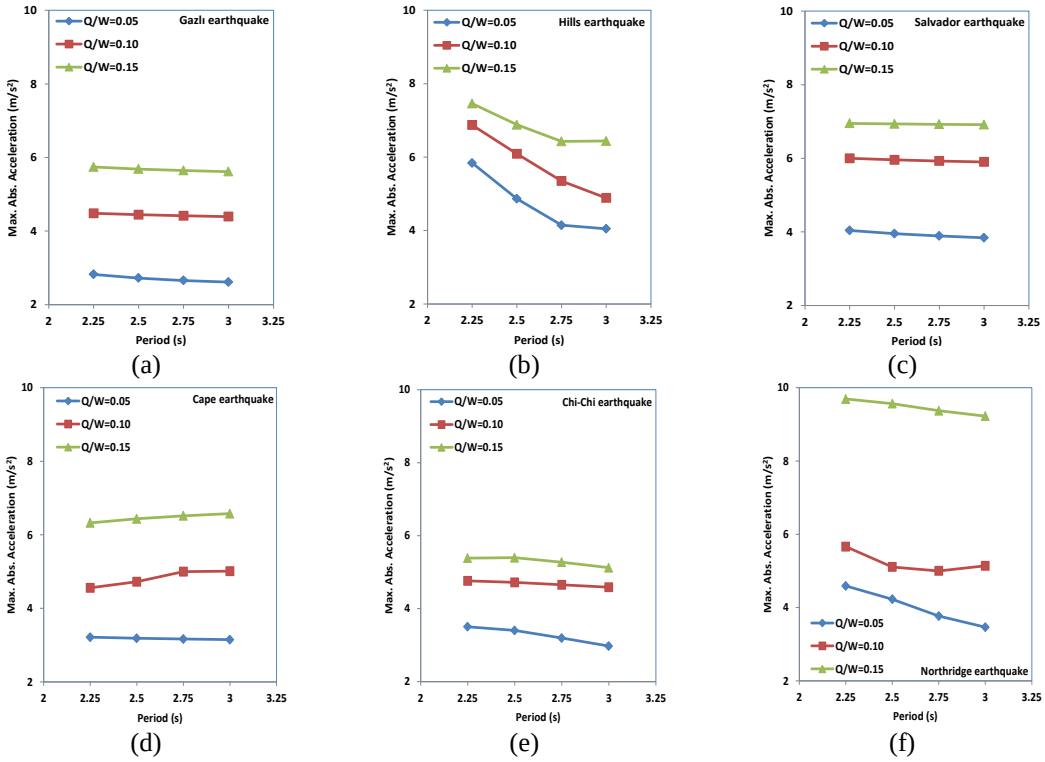

Fig. 11 Variation of maximum absolute acceleration with isolation period and damping of 5-storey SMF under earthquakes

towards the roof storey. For 5 and 10-storey seismically isolated frames, on the average roof absolute acceleration being 1.29 and 1.60 times that of first storey, respectively. The lowest ratio was observed as 1.18 (i.e., 18% increase) in case of T3QW5 for 5-storey isolated frame while 1.29 (i.e., 29% increase) in case of T2.75QW5 for 10-storey isolated frame. The greatest ratio was obtained as 1.44 (i.e., 44% increase) in case of T2.25QW15 for 5-storey isolated frame. Similar trend was observed in the previous studies (Alhan and Sahin, 2011) that was for 6-storey building while 1.87 (i.e., 87% increase) in case of T2.5QW15 for 10-storey frame. At a glance, it was seen that the variation of

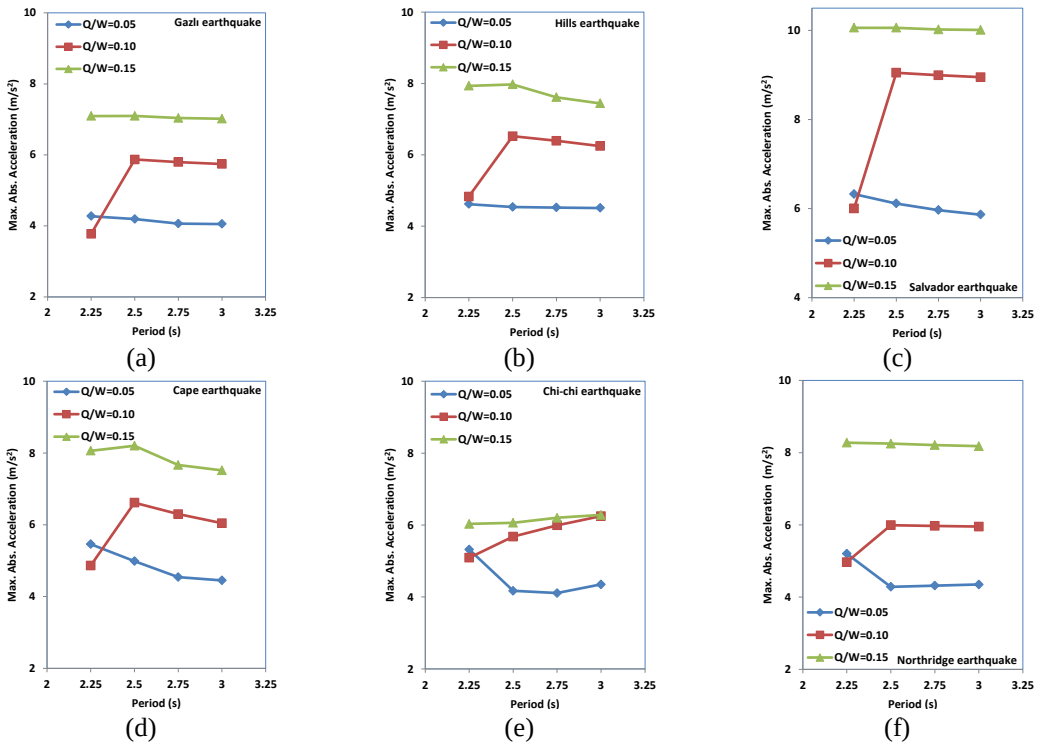

Fig. 12 Variation of maximum absolute acceleration with isolation period and damping of 10-storey SMF under earthquakes

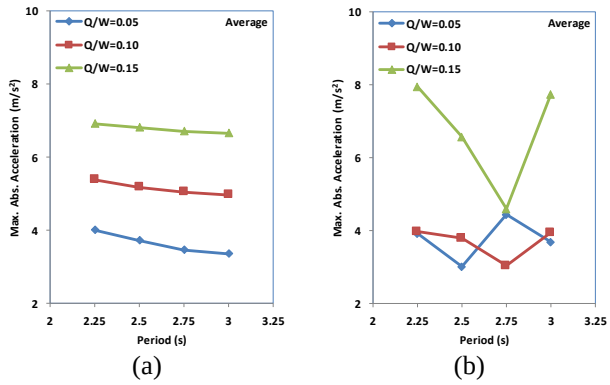

Fig. 13 Variation of average maximum absolute acceleration of 5-storey SMF(left) and 10-storey SMF (right)

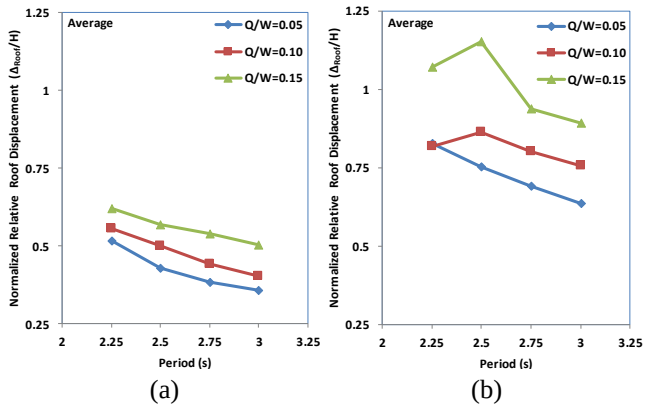

Fig. 14 Variation of average normalized relative roof displacements of 5-storey SMF(left) and 10-storey SMF (right)

the yield strength ratio was dramatically affected the reduction of the roof absolute accelerations when 5-storey seismically isolated frames subjected to Northridge earthquake as shown in Fig. 11(f). For instance, the isolation system of T3QW15 led to 9.225 m/s^2 of roof absolute acceleration while it was reduced up to 3.46 m/s^2 of T3QW5. The corresponding average maximum absolute acceleration values of the isolation system can be observed in Fig. 13 as well. The average and maximum absolute accelerations of both frames with isolation period and yield strength ratio were also given in Figs. 11-13. It was observed that reduction of the yield strength ratio remarkably caused to mitigate the maximum absolute acceleration in all cases and both frames regardless of the earthquake characteristics. Furthermore, increase on the isolation period reflected the similar response for 5-storey base-isolated frames as shown in Figs. 11 and 13(a). However, for 10-storey base-isolated frames the variation of the maximum absolute acceleration was not steady and partially changed with earthquake characteristics as shown in Figs. 12 and 13(b). For instance, the average maximum absolute acceleration was reduced when the isolation period was varied from 2.25 s to 2.75 for corresponding yield strength ratios (namely 0.10 and 0.15) as shown in Fig. 13(b), on the contrary increase of isolation period from 2.75 s to 3 s enhanced the average maximum absolute acceleration. However, for 10-storey base-isolated frames the variation of the maximum absolute acceleration was not steady and partially changed with earthquake characteristics as shown in Figs. 12 and 13(b). For instance, the average maximum absolute acceleration was reduced when the isolation period was varied from 2.25 s to 2.75 for corresponding yield strength ratios (namely 0.10 and 0.15) as shown in Fig. 13(b), on the contrary increase of isolation

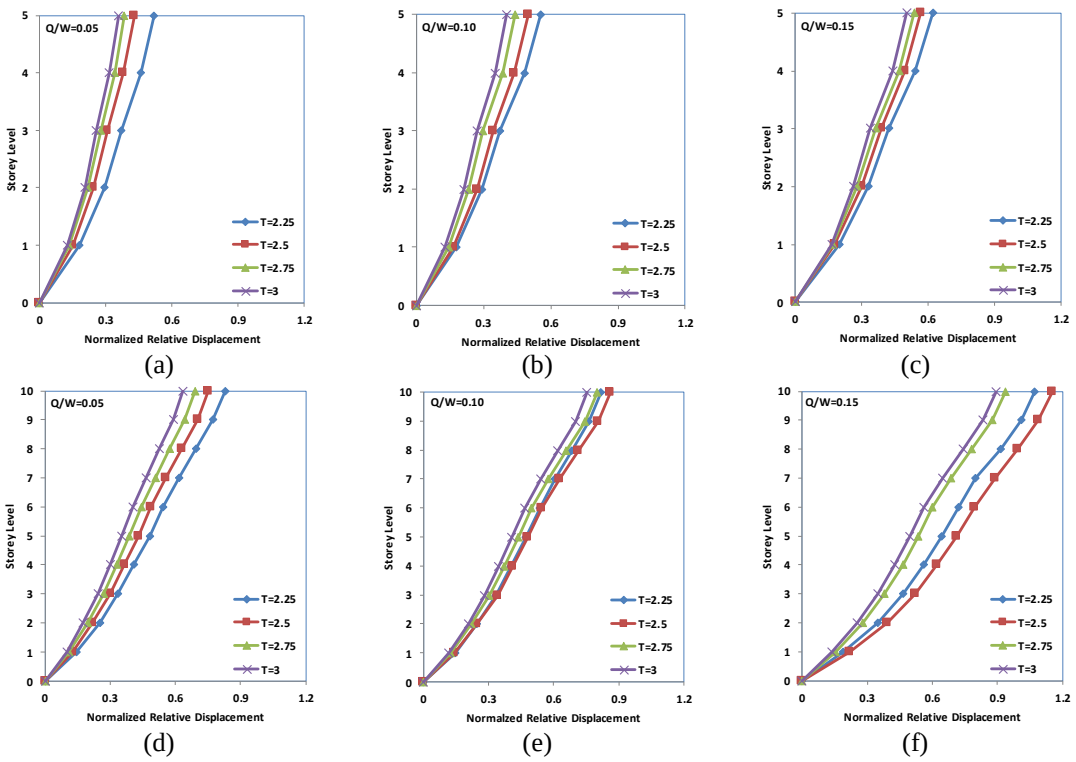

Fig. 15 Variation of average normalized relative displacements with isolation period and damping of 5-storey SMF(left) and 10-storey SMF(right)

period from 2.75 s to 3 s enhanced the average maximum absolute acceleration.

3.3 Relative displacement

The effect of the isolation period and the yield strength ratio on the roof displacement was discussed in section 3.1, but it was exhibited adverse trend in some cases due to the characteristics of the seismic ground motions. Hence, the relative displacement is evaluated as a more efficient criterion and remarkable parameter in the evaluation of the base-isolated steel frames' effectiveness. The relative displacement is equal to the difference between the roof displacement and base displacement (i.e., isolation system displacement). It was also normalized with corresponding storey height and illustrated the average normalized relative roof displacements in Fig. 14. Since the greater isolation period and smaller yield strength ratio presented the lower stiffness value on the isolation systems (see Table 1), in the condition that was enabled to easily lateral movement. It was clearly observed that the increase of the isolation period and the decrease of the yield strength ratio ended up with significant reduction on the normalized relative roof displacement, especially for 5-storey SMF. Fig. 15 showed the variation of the normalized average relative displacements over the height of both isolated frames over the height of both isolated frames considering with the isolation period and yield strength ratio. As explained previously, since the stiffness of the rubber was low, it provided horizontal flexibility and allowed to lateral movement at the base, thus LRB effectively reduced the relative displacement. The relative displacements of 5 and 10-storey seismically isolated frames were computed accordance with the corresponding earthquake motions through nonlinear analysis and it can be clearly observed that the base-isolated frames with different isolation parameters had slightly influenced the variation of the relative displacement. However, the number of the storey and the earthquake characteristic remarkably average relative displacement while the increase of the isolation period seemed to mitigate the average relative displacements for both isolated frames. For instance, increasing the yielding strength enhanced the varied the relative displacement. The most significant reduction in the relative displacement experienced when 5-storey base-isolated frames subjected to Salvador earthquake. The relative displacement demand on the isolation system of T3QW15 was 9.33 cm while it was reduced up to 3.31 cm by T3QW5. It can also be verified that T3QW5 caused minimum average relative displacement response for both frames as shown in Fig. 14. It was conspicuously observed that distribution of the response of the relative displacement was almost tended uniformly stable and similar for both isolated frames in particular 5-storey frame with LRB.

3.4 Interstorey drift

The maximum interstorey drift ratio was a significant parameter directly related to the level of structural damage that may be observed in a structure. Interstorey drift was computed as the difference between displacements of the two consecutive stories normalized by the corresponding storey height. The variation of average interstorey drift versus storey height of 5 and 10-storey isolated frames was

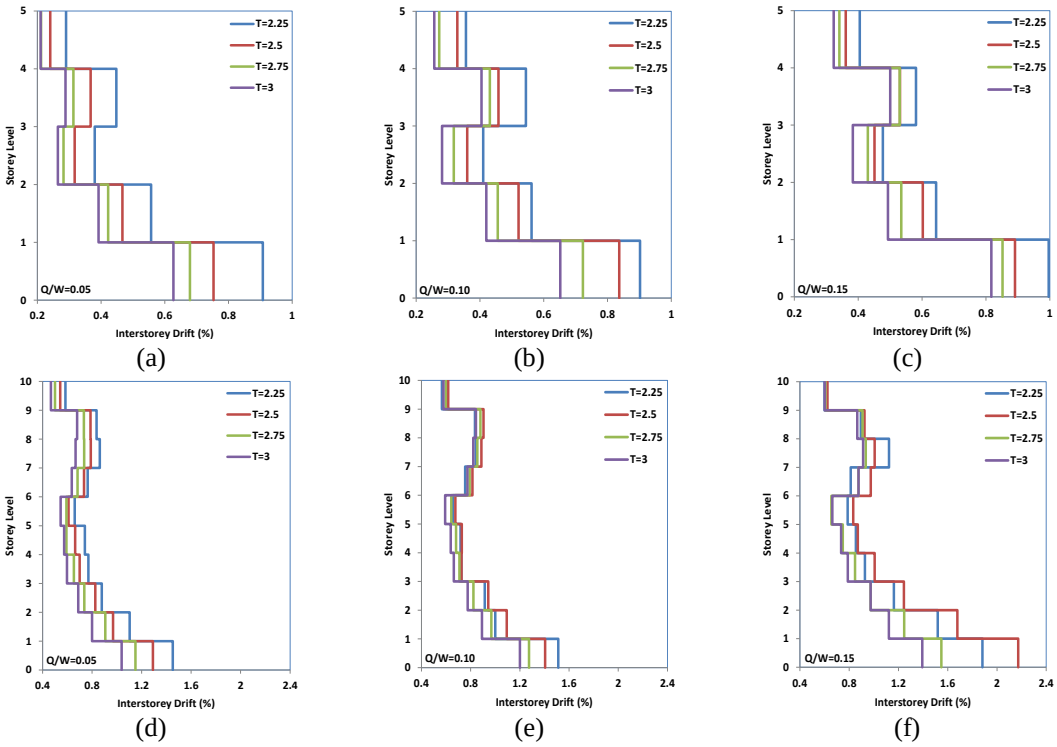

Fig. 16 Variation of average interstorey drift ratio against storey height of 5-storey SMF(left) and 10-storey SMF (right)

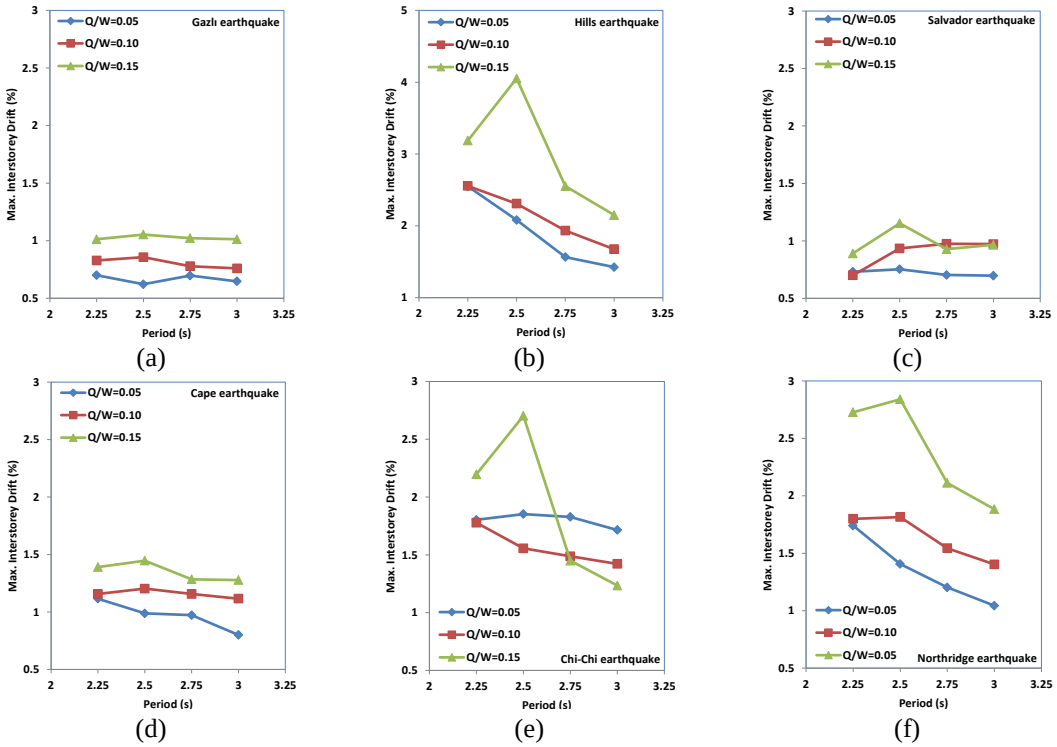

Fig. 17 Variation of maximum interstorey drift ratio with isolation period and damping of 10-storey SMF under earthquakes

plotted in Fig. 15, regarding the isolation parameters (i.e the isolation period and yield strength ratio). The maximum interstorey drift demand of the 5 and 10-storey isolated frames with corresponding isolation period and yield strength ratio under six ground motions were given in Figs. 16-17, respectively. The variation of the average maximum interstorey drift was also plotted in Fig. 18. Firstly, increasing the isolation period seemed to reduce the interstorey drift and distribution of it also tended to behave more uniform over the height of both isolated frames, on the contrary, increasing *Q/W* ratio generally increased the maximum intestorey drift (see Fig. 15). Secondly, it can be clearly seen that 5-storey frames supported with LRB that had various isolation parameters and each of them generally

exhibited similar response under the seismic excitations as shown in Figs. 15-16, on the contrary 10-storey isolated frames did not have a steady response as shown in Figs. 15 and 17. Figs. 15-18 obviously illustrated that interstorey drift ratio was differently influenced with the yield strength ratio (*Q/W*), isolation period (*T*), characteristic of the earthquakes and number of the storey; accordingly, higher yield strength ratio results in either higher or lower interstorey drift depending on the type of earthquake. For example, while the maximum interstorey drift for isolation systems of *T*=2.25 s were significantly lower than those with *T*=2.5 s under Salvador earthquake (see Fig. 17(c)), this behavior was conversed under Northridge earthquake (see Fig. 17(f)) where isolation systems with *T*=2.25 s produce generally higher maximum interstorey drift ratio was differently influenced by the yield strength ratio. On the other hand, higher yield levels (Q/W ratios) typically resulted in higher interstorey drift. An example of the exception is *T*=2.5 s isolation systems with *Q/W*=10% which resulted in slightly lower interstorey drift as compared to those with *Q/W*=5% under Chi-chi earthquake (see Fig. 17(e)). Finally, the isolation system of T3QW5 testified that the lowest reduction in the average maximum interstorey drift which was 0.62 and 1.03% for 5 and 10-storey base-isolated frames as shown in Figs. 18(a)-(b), respectively. All values were smaller than 3% determined as design limit of SMF, and verified the improved effects of the base-isolated system.

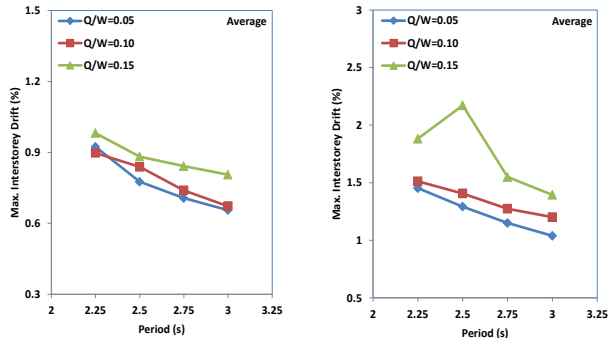

(a) (b)

Fig. 18 Variation of average maximum interstorey drift ratio of 5-storey SMF(left) and 10-storey SMF (right)

3.5 Base shear

The base shear demand of the examined frames was normalized by the building weight and depicted in Figs. 19-21. The use of LRB remarkably reduced the base shear especially 5-storey isolated frames. When each of these isolated frames subjected to the ground motions their responses were obtained and clearly presented in Fig. 19. Besides the variation of the yield strength ratio from 0.15 to 0.05, shifting the isolation period from 2.25 s to 3 s also caused a steady reduction on the base shear as shown in Figs. 19-21(a). Additionally, almost similar responses were valid for 10-storey isolated frames as well (see Figs. 20-21(b)). However, an amplification trend was observed on the base shear demand of 10-storey isolated frames when the isolation period varied from 2.25 s to 2.5 s with corresponding yield strength ratio of 0.10 and 0.15. Furthermore, on behalf of normalizing the base shear with the weight of isolated frames the base shear demand rank between 0.15-0.3 both frames. When T3QW5 was implemented for 5 and 10-storey frames as isolation system that ensured the lowest base shear demand with respect to the other isolation systems as depicted in Figs. 19-21. The

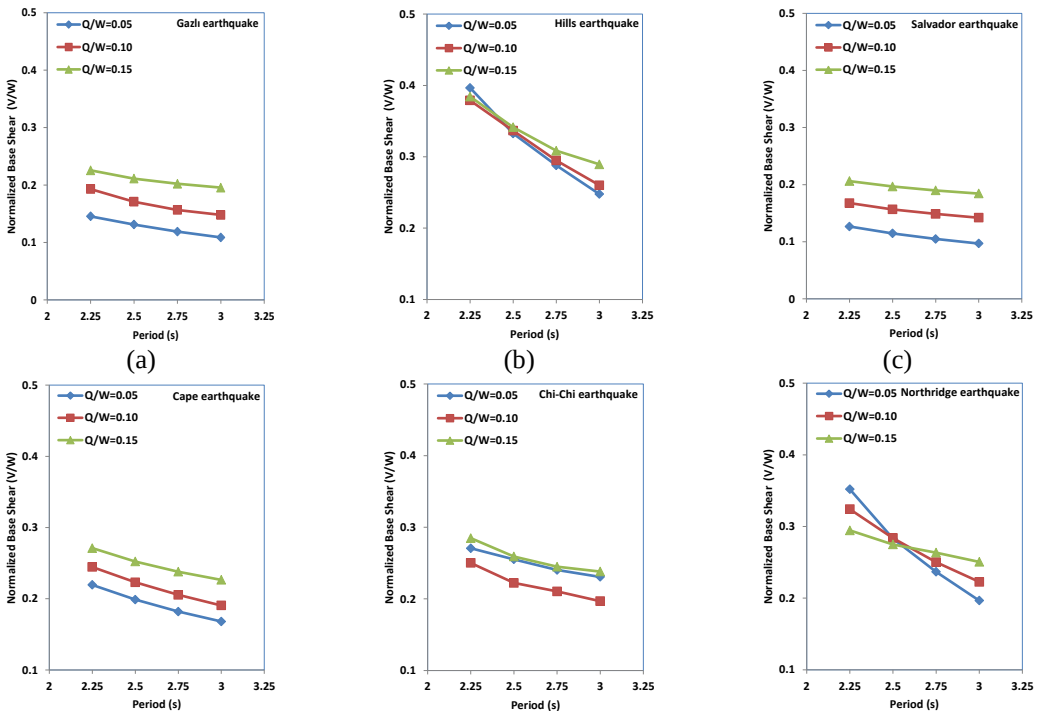

(a) (b) (c)

(d) (e) (f)

Fig. 19 Variation of base shear with isolation period and damping of 5SMF under earthquakes

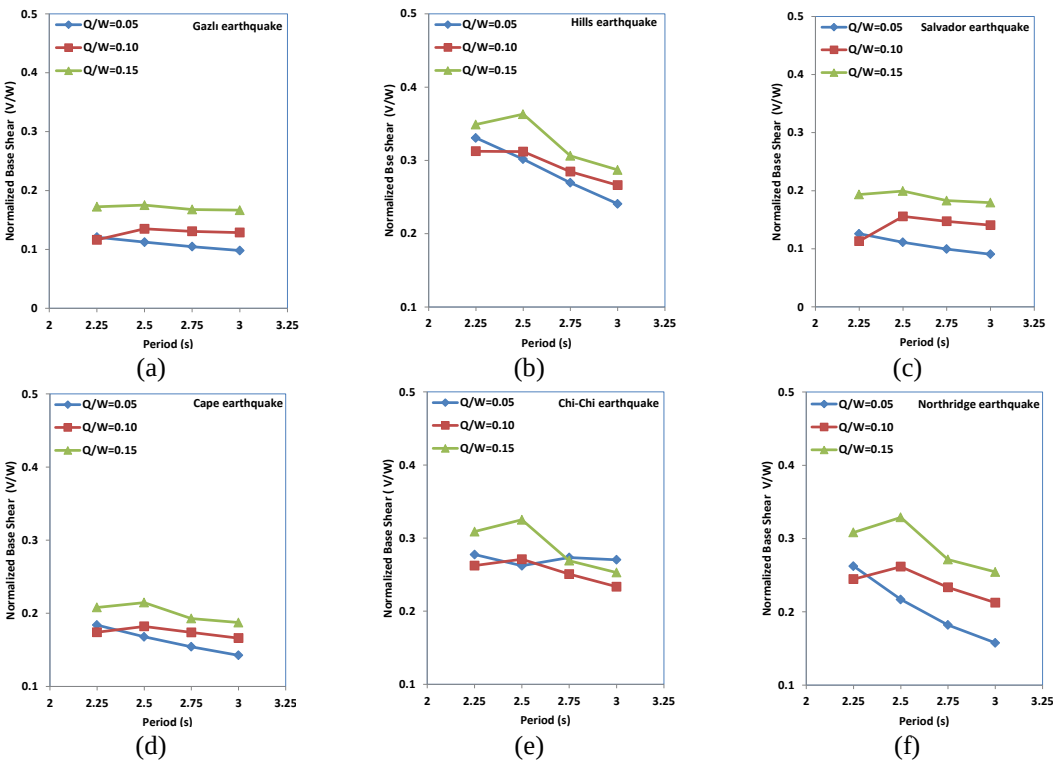

Fig. 20 Variation of base shear with isolation period and damping of 10-storey SMF under earthquakes

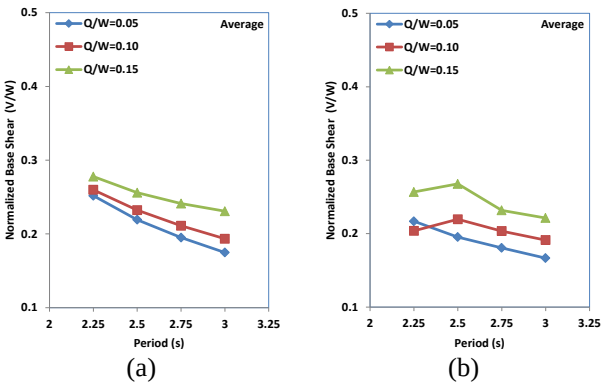

Fig. 21 Variation of average base shear with isolation period and damping of 5-storey SMF(left) and 10-storey SMF (right)

most remarkable behavior was observed under Salvador earthquake, 5 and 10-storey frame with the isolation system of T3QW5 introduced the lowest base shear of 0.096(131.6 kN) and 0.09(352.7 kN), respectively. It should also be noted that the aforementioned nonlinear analysis results on the base shear demand of the examined frames did not differentiate with the earthquake characteristics.

3.6 Hysteretic curve

The hysteretic curves of twelve isolation systems including different isolation period and yield strength ratio for 5 and 10-storey frames under Northridge earthquake were plotted in Fig. 22. These curves were similar to the bi-linear force-deformation as depicted in Fig. 4 (Ö zdemir and Constantinou, 2010). The hysteretic curve of the isolation systems shifted while it abided by the original force-deformation curve. Among the isolation systems, the isolation period of 2.25 s and 3 s, namely had smallest and largest hysteresis curves, and the others remained between them. Since the isolator stiffness of T3QW5 was lower than other isolation systems (see Table 1), it provided horizontal flexibility and allowed to easily lateral movement at the base. For this, the greatest displacement demand of 373 and 378 mm was observed in the isolation system of T3QW5 for 5 and 10-storey SMF which was hit by Northridge earthquake, respectively, as depicted in Fig. 22(a) and (d). It was clearly observed that the decrease of the isolation period and increase of the yield strength ratio led to a reduction of the excessive isolator displacement demand of the 5 and 10-storey SMF. Consequently, the displacement demand of the isolation systems may adjust by altering the isolation parameters (i.e., the isolation period and yield strength ratio).

3.7 Dissipated energy

The higher isolation period and lower yield strength ratio presented the maximum energy dissipation. The amount of dissipated energy by isolators can be determined by Eq. (7) (NEHRP Provisions,2010);

$$E_{loop} = 4(D_{max}F_y - F_{max}D_y) \tag{7}$$

The amount of the dissipated hysteresis energy of each isolation systems under Northridge earthquake presented in Table 3. The highest isolation period and lowest yield strength ratio, T3QW5, ensured the greatest hysteresis energy dissipation of 31.93, 91.76 kNm, respectively for 5

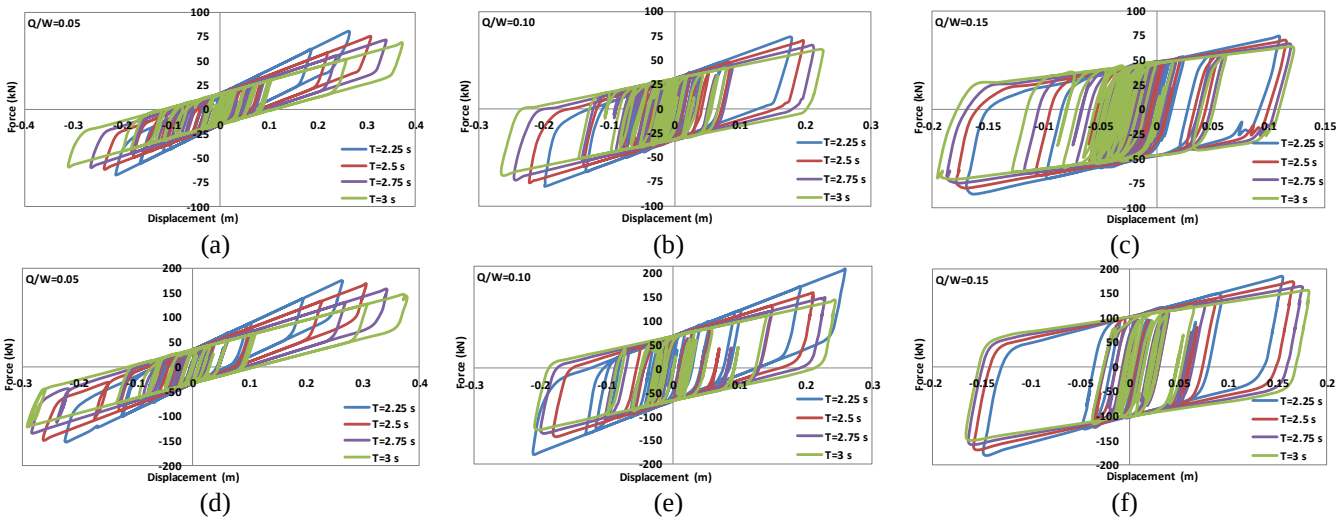

Fig. 22 Bi-linear force-deformation relation of 5-storey SMF (a-b-c) and 10-storey SMF (d-e-f) LRB under Northridge earthquake

Table 3 Total dissipated energy of the isolated frames.

Isolation System	5-Storey E_{loop} (kNm)	10-Storey E_{loop} (kNm)
T2.25QW5	17.64	51.14
T2.25QW10	15.84	45.65
T2.25QW15	6.58	19.05
T2.5QW5	21.98	63.46
T2.5QW10	19.75	57.02
T2.5QW15	8.29	23.95
T2.75QW5	26.57	77.08
T2.75QW10	23.54	68.05
T2.75QW15	9.13	26.38
T3QW5	31.93	91.76
T3QW10	28.14	81.10
T3QW15	10.98	31.63

and 10-storey frame under Northridge earthquake. It was clearly observed that when the yield strength ratio was fixed, the dissipated energy by isolators enhanced with the increase of the isolation period, on the other hand, it decreased with the increase of the yield strength ratio in case of the isolation period remained constant. Ultimately, the effectiveness of the isolation systems can be very easily tuned by conducting the suitable isolation parameters of LRB, namely the isolation period and yield strength ratio.

4. Conclusions

The present analytical work showed that the effect of the isolation period, *T*, and characteristic strength to weight ratio, *Q/W* on the design of base-isolated frame subjected to six natural accelerograms compatible with seismic hazard levels of 2% probability of exceedance in 50 years were considered.

It can be clearly observed that the reduction on the yield strength ratio and the isolation period led to lessening the absolute acceleration, relative displacement, interstorey drift ratio, base shear and the amount of the dissipated energy especially for 5-storey SMF hit by Northridge and Salvador earthquake. However, it should be noted that the results obtained from this study generally depend on the responses of the seismic ground motions, hence the seismic response of the examined frames can be influenced by the differentiation of the characteristics of the earthquakes. In this sense, a wide range of isolation periods and yield strength ratios considering the selection of the earthquake parameters (i.e., bidirectional waves, near and far fault effects) should be regarded to better understand the effectiveness of LRBs on the steel frames for future works. The following conclusions inferred from this study were elaborately explained below:

- Besides the isolation period and yield strength ratio, the characteristic of the earthquakes and the number of storey also had significant effect on the response of the isolated frames.
- It can be revealed that both increasing the isolation period and yield strength ratio generally reduce the roof displacements, however, this reduction easily changed with the type of frames and earthquakes (see Figs. 5-7). Further, the isolation system of T3QW15 presented the lowest average normalized roof displacement of 1.69 (27.16 cm), 1.44 (46.11 cm) for both 5 and 10-storey isolated frames, respectively.
- When the yield strength ratio reached the minimum value of 0.05, the lowest absolute acceleration was obtained for both examined frames. The amplification of the isolation periods triggered the absolute acceleration reduction for the 5-storey frame while for 10-storey isolated frames as the isolation period increased up to 2.75 s, the absolute acceleration was typically reduced and then the variation of isolation period from 2.75 s to 3 s showed counterproductive effect. Further, the lowest absolute accelerations were observed at the mid-storey while the highest absolute acceleration was observed uppermost and then at the lowermost storey where supplemental damping devices must be inserted, the mid-height with the lowest accelerations could be regarded the safest place for the seismic control.

• It was found that the use of LRB with the isolation system with T3QW5 exhibited the most uniform drift distribution and relative displacement. Additionally, the isolation system of T3QW5 presented the lowest interstorey drift and relative displacement values for each frame and ground motions.

• Both increasing the isolation period and yield strength ratio remarkably led to considerable reductions in the base shear. The lowest base shear values were observed in the isolation system of T3QW5 irrespective of the number of storey and earthquake characteristics.

• The use of appropriate isolation systems remarkably caused the most substantial dissipation of the hysteresis earthquake energy.

• To achieve sufficient reduction of the displacements and acceleration under earthquake loads, T3QW5 generally seemed to be the most favorable model.

References

Alhan, C. and Davas, S.Ö. (2016), "Performance limits of seismically isolated buildings under near-field earthquakes", *Eng. Struct.*, **116**, 83-94.

Alhan, C. and Şahin, F. (2011), "Protecting vibration-sensitive contents: An investigation of floor accelerations in seismically isolated buildings", *Bull. Earthq. Eng.*, **9**, 1203-1226.

Alhan, C. and Sürmeli, M. (2011), "Shear building representations of seismically isolated buildings", *Bull. Earthq. Eng.*, **9**, 1643-1671.

ASCE (1998), Evaluation Findings for Skellerup Base Isolation Elastomeric Bearings, Technical Evaluation Report, CERF Report: HITEC 98-12, Prepared by the Highway Innovative Technology Evaluation Center.

ASCE 41-06 (2006), Seismic Rehabilitation of Existing Buildings, American Society of Civil Engineers, Reston.

ASCE 7-05 (2005), Minimum Design Loads for Buildings and Other Structures, American Society of Civil Engineers, Reston, Virginia.

Asgarian, B., Sadrinezhad, A. and Alanjari, P. (2010), "Seismic performance evaluation of steel moment resisting frames through incremental dynamic analysis", *J. Constr. Steel Res.*, **66**(2), 178-190.

Bilgin, H. (2013), "Fragility-based assessment of public buildings in Turkey", *Eng. Struct.*, **56**, 1283-1294.

Building Seismic Safety Council (2010), NEHRP Recommended Provisions for Seismic Regulations for New Buildings and other Structures, FEMA Engineers, Reston, Virginia.

Chun, Y.S. and Hur, M.W. (2015), "Effects of isolation period difference and beam-column stiffness ratio on the dynamic response of reinforced concrete buildings", *Int. J. Concrete Struct. Mater.*, **9**(4), 439-451.

Computers and Structure (2011), Inc., SAP 2000 Advanced 14.0.0, Structural Analysis Program, Berkeley, CA.

Das, S. and Mishra, S.K. (2014), "Optimal performance of buildings isolated by shape-memory-alloy-rubber-bearing (SMARB) under random earthquakes", *Int. J. Comput. Meth. Eng. Sci. Mech.*, **15**(3), 265-276.

Das, S., Gur, S., Mishra, S.K. and Chakraborty, S. (2015), "Optimal performance of base-isolated building considering limitation on excessive isolator displacement", *Struct. Infrastr. Eng.*, **11**(7), 904-917.

Erkal, A., Tezcan, S.S. and Debra, F. and Laefer, D.F. (2011), "Assessment and code considerations for the combined effect of seismic base isolation and viscoelastic dampers", *ISRN Civil Eng.*, **2011**, 10.

Etedali, S. and Sohrabi, M.R. (2016), "A proposed approach to mitigate the torsional amplifications of asymmetric base-isolated buildings during earthquakes", *J. Civil Eng.*, **20(2)**, 768-776.

FEMA (2000), Prestandard and Commentary for the Seismic Rehabilitation of Building, Federal Emergency Management Agency, 356, Washington, D.C.

FEMA (2000), Seismic Design Criteria for New Moment-Resisting Steel Frame Construction, Federal Emergency Management Agency, Washington, D.C.

Fragiacomo, M., Rajgelj, S. and Cimadom, F. (2003), "Design of bilinear hysteretic isolation systems", *Earthq. Eng. Struct. Dyn.*, **32**(9), 1333-1352.

Fujita, T. (1998), "Seismic isolation of civil buildings in Japan", *Prog. Struct. Eng. Mater.*, **1**(3), 295-300.

Gur, S. and Mishra, S.K. (2013), "Multi-objective stochastic-structural-optimization of shape-memory-alloy assisted pure-friction bearing for isolating building against random earthquakes", *Soil Dyn. Earthq. Eng.*, **54**, 1-16.

Hameed, A., Koo, M.S., Do, T.D. and Jeong, J.H. (2008), "Effect of lead rubber bearing characteristics on the response of seismic-isolated bridges", *J. Civil Eng.*, **12**(3), 187-196.

Jangid, R.S. (2007), "Optimal lead-rubber isolation bearings for near-fault motions", *Eng. Struct.*, **29**, 2503-2513.

Jerome, J.C. (2002), *Introduction to Structural Motion Control*, Massachusetts Institute of Technology, Pearson Education, Inc., Upper Saddle River, New Jersey.

Khoshnudian, F. and Motamedi, D. (2013), "Seismic response of asymmetric steel isolated structures considering vertical component of earthquakes", *J. Civil Eng.*, **17**(6), 1333-1347.

Kulkarni, J.A. and Jangid, R.S. (2003), "Effects of superstructure flexibility on the response of base-isolated structures", *Shock Vib.*, **10**(1), 1-13.

Liang, B., Shishu, X. and Jiaxiang, T. (2002), "Wind effects on habitability of base-isolated buildings", *J. Wind Eng. Indus. Aerodyn.*, **90**(12-15), 1951-1958.

Liu, T., Zordan, T., Briseghella, B. and Zhang, Q. (2014), "An improved equivalent linear model of seismic isolation system with bilinear behavior", *Eng. Struct.*, **61**, 113-126.

Matsagar, V.A. and Jangid, R.S. (2004), "Influence of isolator characteristics on the response of base-isolated structures", *Eng. Struct.*, **26**(10), 1735-1749.

Naeim, F. and Kelly, J.M. (1999), *Design of Seismic Isolated Structures, From Theory to Practice, Shock and Vibration*, John Wiley & Sons, New York, NY, USA.

Nigdeli, S.M., Bekdaş, G. and Alhan C. (2014), "Optimization of seismic isolation systems via Harmony search", *Eng. Optim.*, **46**, 1553-1569.

Özdemir, G. and Akyüz, U. (2012), "Performance of a multi-story isolated building subjected to bidirectional excitations in protection of critical equipments from earthquake hazard", *15th World Conference on Earthquake Engineering*, Lisboa, Portugal.

Özdemir, G. and Bayhan, B. (2015), "Response of an isolated structure with deteriorating hysteretic isolator model", *Res. Eng. Struct. Mater.*, **10**, 1-10.

Ö zdemir, G. and Constantinou, M.C. (2010), "Evaluation of equivalent lateral force procedure in estimating seismic isolator displacements", *Soil Dyn. Earthq. Eng.*, **30**(10), 1036-1042.

Park, Y.J., Wen, Y.K. and Ang, A.H.S. (1986), "Random vibration of hysteretic systems under bi-directional ground motions", *Earthq. Eng. Struct. Dyn.*, **14**(4), 543-557.

PEER (2011), User's Manual for the PEER Ground Motion Database Application, The Pacific Earthquake Engineering Research Center, University of California, Berkeley.

Providakis, C.P. (2008), "Pushover analysis of base-isolated steel–

concrete composite structures under near-fault excitations", *Soil Dyn. Earthq. Eng.*, **28**, 293-304.

Ryan, L. and Chopra, A.K. (2004), "Estimation of seismic demands on isolators based on nonlinear analysis", *J. Struct. Eng.*, ASCE, **130**(3), 392-402.

Vasiliadis, L.K. (2016), "Seismic evaluation and retrofitting of reinforced concrete buildings with base isolation systems", *Earthq. Struct.*, **10**(2), 293-311.

CC